

The Stir–Settle Approach to Semiautomated Light Scattering Determination of Liquid–Liquid Coexistence Curves

Kevin M. Dean[†] and J. Charles Williamson*

Department of Chemistry, Willamette University, 900 State Street, Salem, Oregon 97301, United States

ABSTRACT: Critical opalescence turbidity masks the precise location of liquid–liquid coexistence curve temperatures (T_{cx}) in light scattering data collected from stirred samples using semiautomated instrumentation. A modified semiautomated technique in which a stirred sample is fully equilibrated and then light scattering data is collected as a function of time with no stirring is described. Tests on three systems (aniline + hexane, methanol + cyclohexane, and isobutyric acid + water) showed that coalescence and sedimentation in the unstirred two-phase sample causes distinct temporal changes in the light scattering, most noticeably in light collected 2° off-incidence. With this experimental method, the coexistence curve temperatures of near-critical samples can be identified with ± 0.01 K uncertainty. Precise determination of T_{cx} can also be hampered by long mixing times. Equilibration lag measurements as a function of sample composition and ramping rate are also reported. These measurements show that the equilibration lag increases as the system composition moves away from the critical composition. In addition, the lag is asymmetric with respect to T_{cx} : equilibration of two phases into one phase requires more time (and results in a greater lag) than separation of one phase into two phases.

INTRODUCTION

Careful determination of the temperature/composition coexistence curves for partially miscible binary liquid systems enhances the basic understanding of chemical mixing interactions and is important for the optimization of chemical engineering processes. For example, there is significant interest at present in the characterization of binary liquid systems involving ionic liquids because of the potential of these systems to be used as “greener” solvents.^{1–4} Efforts to streamline the process of measuring liquid–liquid coexistence curves are largely based on the synthetic method,⁵ in which many samples are prepared in order to span the composition coordinate and then the coexistence curve temperature T_{cx} of each sample is determined individually. Most semiautomated instrumentation described in the literature for synthetic method analysis uses optical techniques for the identification of T_{cx} .^{6–17} Transmitted or scattered light from a stirred sample is recorded as a function of temperature, and a change in this signal is associated with a change in sample turbidity (the cloud point) that is expected to accompany phase separation. Values of T_{cx} determined by this method have frequently been reported with 0.01 K precision.

We recently pointed out limitations on the accuracy to which T_{cx} can be assigned using the semiautomated light scattering technique.¹⁸ For samples with compositions near the critical composition, the uncertainty in T_{cx} values found solely from the evaluation of transmitted or scattered light from stirred samples is actually limited to ± 0.05 K by turbidity contributions from critical opalescence. Furthermore, some common T_{cx} assignment methods can result in systematic errors of 0.2 K or more when applied to light scattering data from near-critical samples. Alternative time-consuming techniques, such as manual observation of the spinodal decomposition diffraction ring,^{19,20} are necessary to attain ± 0.01 K uncertainty. We also noted evidence for very

long mixing times in some samples, leading to a lag in equilibration and an incorrect assignment of T_{cx} . Equilibration lags were observed even though the effective rate of our temperature ramping was only $20 \mu\text{K}\cdot\text{s}^{-1}$, which was 1 to 2 orders of magnitude lower than the rates reported for most other similar experiments.

Here we describe a modified approach for the determination of T_{cx} in liquid–liquid mixtures using semiautomated instrumentation. After collecting light scattering signals from a stirred sample in the usual way, we stop the stirring and continue to monitor the light signals, allowing the two-phase systems to settle through droplet coalescence and gravitational sedimentation. Tests were conducted on three systems with varied opalescence strength: aniline + hexane, methanol + cyclohexane, and isobutyric acid + water. We show that the stir–settle method eliminates the ambiguity in the assignment of T_{cx} from light scattering data for near-critical samples for all of these systems. We also report the results of a survey of the equilibration lag in these three systems as a function of sample composition and temperature ramping rate. This survey shows how and to what magnitude the equilibration lag manifests in semiautomated instrumentation data.

EXPERIMENTAL DETAILS

Sample Preparation. Puriss-p.a.-grade isobutyric acid (0.999 mass fraction) and puriss-p.a.-grade water suitable for inorganic

Special Issue: John M. Prausnitz Festschrift

Received: October 30, 2010

Accepted: January 7, 2011

Published: January 26, 2011

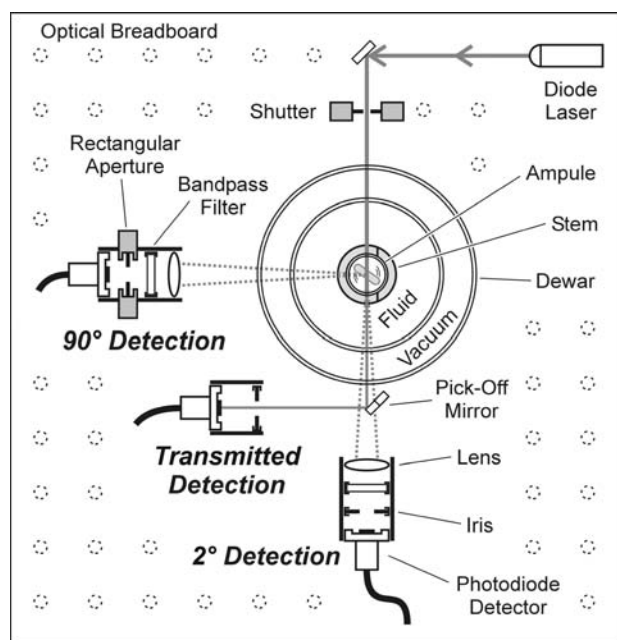


Figure 1. Overhead view of the optics setup for measuring light scattered from a continuously stirred liquid–liquid sample. Detection at 90° was optimized to image just the laser path through the ampule. The laser was linearly polarized normal to the scattering plane.

trace analysis (0.9999+ mass fraction) were purchased from Fluka. Colorless ACS-reagent-grade aniline (0.999 mass fraction) was purchased from Aldrich and stored in a freezer, and puriss-p. a.-grade hexane standard for GC (0.997 mass fraction) was purchased from Fluka. Anhydrous methanol (0.9999 mass fraction) and anhydrous cyclohexane (0.9999 mass fraction) were purchased from Aldrich and stored over activated molecular sieves. All of the chemicals were used without further purification.

Binary mixtures were prepared by transferring the neat liquids to custom glass ampules using syringes. Each ampule also held a magnetic stir bar. The total volume of liquid inside an ampule was about 2 mL. Each sample was degassed through a series of freeze–pump–thaw cycles, and then the ampule was flame-sealed under vacuum while the contents remained frozen. Mole fraction compositions of the mixtures were determined gravimetrically with uncertainties on the order of a few parts in ten thousand. Compositions were corrected for buoyancy and evaporation into the ampule head space. Finished aniline + hexane and methanol + cyclohexane samples were stored in a standard freezer.

Instrumentation. A detailed description of our light scattering instrumentation has been presented elsewhere.¹⁸ Briefly, each liquid–liquid sample was immersed in a custom clear-glass Dewar connected to a recirculating Neslab water bath (RTE-111). The water bath provided temperature control to a precision of 0.01 K, and the temperature in the Dewar at the sample was monitored with a NIST-traceable thermistor and meter (Omega, ON-410-PP, HH42). The sample was illuminated with 3 mW radiation from a 635 nm diode laser (Thorlabs, CPS196). Transmitted light, light scattered at 2° off-incidence, and light scattered at 90° were collected simultaneously (Figure 1) as a function of temperature using three photodetectors (Thorlabs, PDA520). To stir the sample, the magnetic stir bar inside each ampule was rotated at 10 Hz using through-space coupling to a

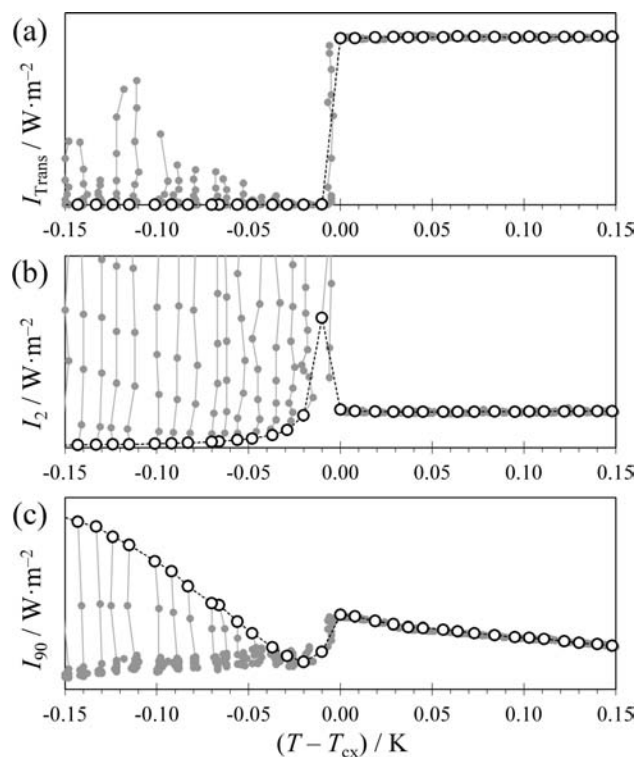


Figure 2. Light scattering data for the aniline + hexane system with $x_{\text{Ani}} = 0.4349$ at temperatures near T_{cx} : \circ , stirred sample; \bullet , data recorded over 30 s intervals after stirring was stopped. (a) Transmitted light intensity, I_{Trans} . (b) Light scattered at 2° , I_2 . (c) Light scattered at 90° , I_{90} .

much larger spin bar in the bottom of the Dewar; the Dewar itself sat on a computer-controlled magnetic stirring plate. Operation of the instrument was automated using programs written with LabView (National Instruments).

Data Collection. The instrumentation had two modes of data collection: stir–settle and ramping. In both modes, data were collected by taking the sample first from the one-phase region into the two-phase region and then back again along the reverse temperature path. In stir–settle mode, the temperature of the water bath was changed in 0.01 K steps. Each step included 420 s for equilibration, 60 s of light signal collection with the laser off, and 60 s of signal collection with the laser on. The stirring plate was then turned off, and light signals were averaged over successive 30 s intervals for 240 s or more of total settling time. Stirring was restarted for the next temperature step. The effective temperature ramping rate in stir–settle mode was between (10 and 20) $\mu\text{K}\cdot\text{s}^{-1}$, depending on the amount of settling time.

In ramping mode, the water bath temperature was changed linearly as a function of time at a rate of (167, 556, or 1670) $\mu\text{K}\cdot\text{s}^{-1}$. Stirring and laser illumination remained on throughout the experiment. Light signals were averaged over intervals of (60, 20, or 10) s (depending on the ramp rate) to provide a data point once every (10 to 20) mK.

RESULTS AND DISCUSSION

Stir–Settle Measurements. In our earlier work, we observed that T_{cx} could be most accurately determined for those samples with compositions displaced from the critical composition but still in a region where the slope of the coexistence curve

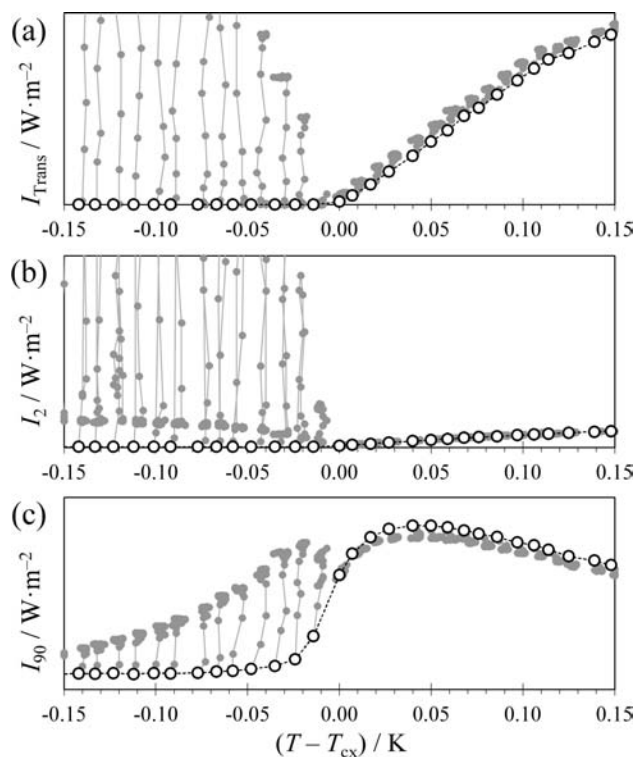


Figure 3. Light scattering data for the aniline + hexane system with $x_{\text{Ani}} = 0.5194$ at temperatures near T_{cx} : \circ , stirred sample; \bullet , data recorded over 30 s intervals after stirring was stopped. (a) Transmitted light intensity, I_{Trans} . (b) Light scattered at 2° , I_2 . (c) Light scattered at 90° , I_{90} .

remained relatively shallow.¹⁸ Interpretation of the light scattering data is straightforward for these samples: substantial droplet formation develops rapidly as the temperature is lowered below T_{cx} , but the critical opalescence turbidity is weak. As an introduction to the stir–settle technique, Figure 2 shows data collected from such a sample: the aniline + hexane system with $x_{\text{Ani}} = 0.4349$. At and above T_{cx} , the cessation of stirring has no effect on the transmitted, 2° , and 90° light signals. Below T_{cx} , all three signals show transient behavior once stirring is stopped, and changes are clearly evident within just 60 s of settling. For this particular sample, the turbidity decreases during settling because nascent-phase droplets are no longer constantly broken up by turbulence, and the droplets begin to coalesce. Since multiple scattering decreases, more Mie-scattered light is collected at 2° , and there is more transmitted light as well. The cumulative settling time for each temperature step in this experiment was 360 s; if the sample were given enough time to complete the sedimentation process, then the transmitted light signal would rise back to its single-phase level because the laser would pass through only one of the two layers.

Although this aniline + hexane sample was displaced from the critical composition, it still exhibited weak opalescence. The 90° data reached a maximum at T_{cx} because of the turbidity of opalescence in the bulk solution (Figure 2c). Below T_{cx} , multiple scattering in the stirred sample caused the 90° scattering to increase with a decrease in temperature, but once the stirring was stopped, the signal rapidly declined to a nonopalescent baseline.

Figure 3 shows stir–settle data for $x_{\text{Ani}} = 0.5194$, a near-critical mixture. T_{cx} was determined independently for this sample by observation of the spinodal decomposition diffraction ring, and

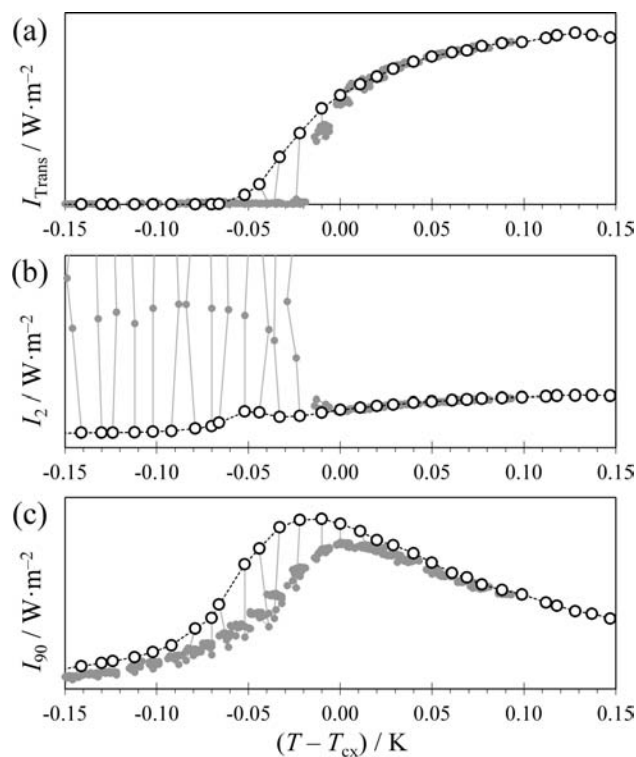


Figure 4. Light scattering data for the isobutyric acid + water system with $x_{\text{IBA}} = 0.1187$ at temperatures near T_{cx} : \circ , stirred sample; \bullet , data recorded over 30 s intervals after stirring was stopped. (a) Transmitted light intensity, I_{Trans} . (b) Light scattered at 2° , I_2 . (c) Light scattered at 90° , I_{90} .

the assignment coincided with the lowest temperature immediately prior to transient behavior in the scattering signals. Of particular importance is the fact that T_{cx} was more than 1 K lower than the onset of the decline in the transmitted intensity signal. Some authors have assigned T_{cx} to this onset of decline (or to the onset of increased off-axis light scattering), but Figure 3a clearly shows that this assignment is incorrect. Instead, strong critical opalescence caused the amount of transmitted light to decrease while the sample was still a single phase. In fact, the opalescence was so strong in this sample that multiple scattering took place while the sample was still a single phase, and therefore, the measured maximum in the 90° scattering data actually occurred at a temperature above T_{cx} (in this case, about 0.05 K higher). Whereas multiple scattering in stirred, two-phase $x_{\text{Ani}} = 0.4349$ increased the 90° signal (Figure 2c), multiple scattering in stirred, two-phase $x_{\text{Ani}} = 0.5194$ was strong enough to attenuate the 90° signal. The settle data then rose from this level: critical opalescence was present in the two-phase system near T_{cx} because the compositions of the newly formed phases were still relatively close to the critical composition.

The stir–settle data from near-critical isobutyric acid + water ($x_{\text{IBA}} = 0.1187$) were different from the near-critical aniline + hexane data in several ways. First, the densities of isobutyric acid and water are closely matched, and even after 600 s of settling time there was very little sedimentation. As a result, there was no change in the transmitted intensity except just below T_{cx} (Figure 4a). However, the cessation of stirring caused an immediate increase in the 2° signal (Figure 4b), which provides the most vivid evidence for the location of T_{cx} . This value for T_{cx} was confirmed by observation of the spinodal decomposition diffraction ring.

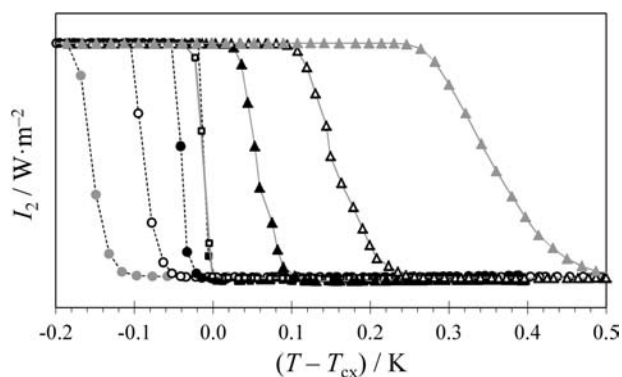


Figure 5. Temperature ramp rate dependence of the 2° light scattering data for the stirred isobutyric acid + water system with $x_{\text{IBA}} = 0.2902$ at temperatures near T_{cx} : gray \bullet , $-1670 \mu\text{K}\cdot\text{s}^{-1}$; gray \blacktriangle , $+1670 \mu\text{K}\cdot\text{s}^{-1}$; \circ , $-556 \mu\text{K}\cdot\text{s}^{-1}$; \triangle , $+556 \mu\text{K}\cdot\text{s}^{-1}$; black \bullet , $-167 \mu\text{K}\cdot\text{s}^{-1}$; black \blacktriangle , $+167 \mu\text{K}\cdot\text{s}^{-1}$; \blacksquare , stepped at an equivalent ramp rate of $-10 \mu\text{K}\cdot\text{s}^{-1}$; \square , stepped at an equivalent ramp rate of $+10 \mu\text{K}\cdot\text{s}^{-1}$.

A second difference between the two systems is that isobutyric acid + water exhibited weaker opalescence than aniline + hexane. The onset of the decline in transmitted intensity occurred only about 0.2 K above T_{cx} (Figure 4a), and T_{cx} itself was in the middle of the decline rather than at the end as in the case of $x_{\text{Ani}} = 0.5194$ (Figure 3a). A third difference is that the location of T_{cx} was actually at a higher temperature than the observed maximum in the 90° scattering data from the stirred sample (Figure 4c). The settle data showed that once stirring was stopped, T_{cx} did occur at the maximum of the 90° data as expected. This offset in the 90° maximum between stirred and unstirred samples is consistent with reports of stirring suppression in the isobutyric acid + water system.²¹

The stir–settle data from a near-critical methanol + cyclohexane sample (not shown) exhibited behavior with characteristics between those of aniline + hexane and isobutyric acid + water. In all three systems, T_{cx} could be identified from stir–settle data to at least ± 0.01 K, the limit of temperature control with our instrumentation. This is in contrast to an analysis based on just the stirred data alone. An uncertainty of ± 0.01 K in T_{cx} was not possible in the latter case, as there was no distinct signature associated with the occurrence of the phase transition in either the transmitted, 2° , or 90° data. For example, T_{cx} occurred at a temperature lower than the maximum in the 90° data from the $x_{\text{Ani}} = 0.5194$ sample but at a temperature higher than the maximum in the 90° data from the $x_{\text{IBA}} = 0.1187$ sample. Figures 2 to 4 show that the stir–settle technique clearly resolves this type of interpretational ambiguity.

Equilibration Lag Measurements. A key motivation behind the development of semiautomated instrumentation for the determination of liquid–liquid coexistence curve temperatures is to limit the amount of direct human supervision necessary for the observation of slowly equilibrated chemical behavior. Most instrumentation described in the literature collects light scattering data while the sample temperature is ramped continuously at rates ranging from (167 to 1670) $\mu\text{K}\cdot\text{s}^{-1}$. Figure 5 presents 2° light scattering data for the isobutyric acid + water system with $x_{\text{IBA}} = 0.2902$. At an effective rate of $10 \mu\text{K}\cdot\text{s}^{-1}$, the decreasing and increasing temperature data sets coincided for this sample, indicating that the sample was given sufficient time to equilibrate. However, a ramping rate of $167 \mu\text{K}\cdot\text{s}^{-1}$ was too fast for this sample, even though the total volume was less than 2 mL and the

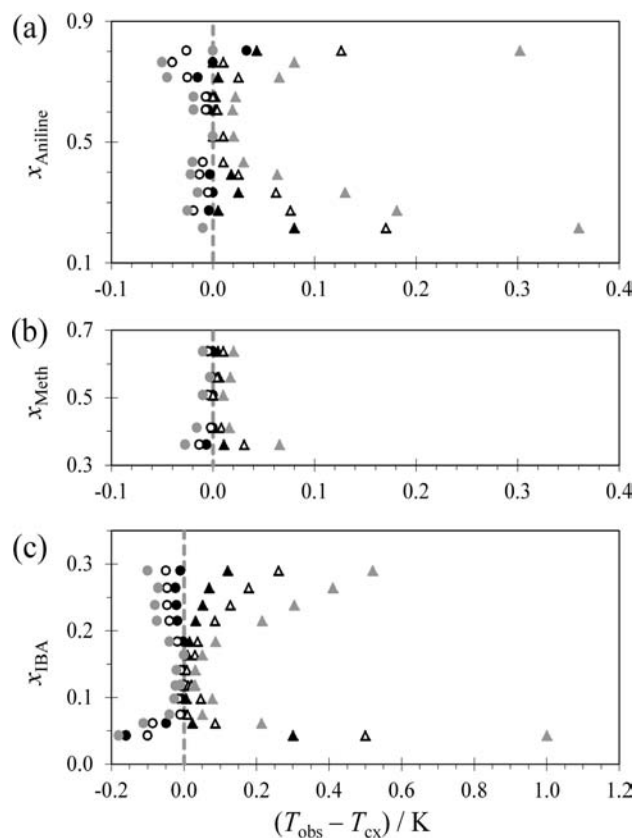


Figure 6. Liquid–liquid equilibration lag, $T_{\text{obs}} - T_{\text{cx}}$ as a function of sample composition and ramping rate. T_{cx} values were determined by stir–settle measurements using effective ramping rates between (10 and 20) $\mu\text{K}\cdot\text{s}^{-1}$. The stir–settle measurements exhibited no equilibration lag. Gray \bullet , $-1670 \mu\text{K}\cdot\text{s}^{-1}$; gray \blacktriangle , $+1670 \mu\text{K}\cdot\text{s}^{-1}$; \circ , $-556 \mu\text{K}\cdot\text{s}^{-1}$; \triangle , $+556 \mu\text{K}\cdot\text{s}^{-1}$; black \bullet , $-167 \mu\text{K}\cdot\text{s}^{-1}$; black \blacktriangle , $+167 \mu\text{K}\cdot\text{s}^{-1}$. (a) Aniline + hexane. (b) Methanol + cyclohexane. (c) Isobutyric acid + water.

sample was vigorously stirred at 10 Hz. As Figure 5 shows, the phase transition on the run of decreasing temperature lagged 0.01 K below T_{cx} , while the phase transition on the run of increasing temperature was not complete until 0.12 K above T_{cx} . The magnitude of equilibration lag increased as the ramping rate increased.

A survey of equilibration lags for three liquid–liquid systems is presented in Figure 6. Equilibration lag was quantified here by the difference between the observed phase transition temperature, T_{obs} , and the coexistence curve temperature T_{cx} determined using stir–settle measurements. The graphs in Figure 6 show the influence of composition and ramping rate on the equilibration lag, and three general trends are important to note. First, all of the samples exhibited some degree of measurable lag for a ramping rate of $1670 \mu\text{K}\cdot\text{s}^{-1}$. Second, the smallest equilibration lag occurred in near-critical samples, and the magnitude of equilibration lag increased as the sample composition moved away from the critical composition. For example, a ramping rate of $167 \mu\text{K}\cdot\text{s}^{-1}$ still caused a lag of 0.1 K or more for samples well-removed from the critical composition. Third, the equilibration lag was asymmetric: there was less lag when a sample separated from one phase into two phases than when the sample recombined from two phases back into a single phase. Some authors have reported T_{cx} as the average of observed values of $T_{\text{cx},1\rightarrow 2}$ and $T_{\text{cx},2\rightarrow 1}$. Figure 6 shows that this average value is likely to be in

error (systematically too high) when the ramping rate is high enough to result in a significant equilibration lag.

CONCLUSIONS

Semiautomated instruments for light scattering determination of liquid–liquid coexistence curve temperatures commonly use temperature ramping, but this technique does not allow T_{cx} to be determined with ± 0.01 K uncertainty for all samples because of the complexity of the light scattering signal in the vicinity of the critical point. We have shown that ± 0.01 K uncertainty is attainable when instrumentation and automation software are designed to step the temperature, let the stirred sample equilibrate, and then record settling data for several hundred seconds with the stirring turned off. We recommend collecting 2° off-incidence scattering data in order to obtain the greatest sensitivity for the occurrence of the phase transition, although valuable complementary information is provided by simultaneously observing the transmitted and/or 90° scattering data. While temperature ramping may be adequate for projects with less demanding requirements on the uncertainty of T_{cx} we have observed that an equilibration lag is common under typical experimental ramping conditions. The lag can be significant (> 0.1 K) for sample compositions displaced from the critical composition. Therefore, we recommend collecting data from both decreasing and increasing temperature ramps in order to monitor the equilibration lag, and we note that the values of $T_{cx,1\rightarrow 2}$ and $T_{cx,2\rightarrow 1}$ may be distributed asymmetrically about the true T_{cx} .

AUTHOR INFORMATION

Corresponding Author

*E-mail: jwillia@willamette.edu.

Present Addresses

[†]Department of Chemistry and Biochemistry, University of Colorado at Boulder, Boulder, CO 80309.

Funding Sources

This work was supported by the National Science Foundation under Major Research Instrumentation Grant 0116713. Undergraduate and faculty summer research stipends were provided by the Mary Stuart Rogers Foundation.

ACKNOWLEDGMENT

The authors thank Elise Helvie for preparation of the methanol + cyclohexane samples.

REFERENCES

- (1) Trindade, C. A. S.; Visak, Z. P.; Bogel-Lukasik, R.; Bogel-Lukasik, E.; Nunes da Ponte, M. Liquid–liquid equilibrium of mixtures of imidazolium-based ionic liquids with propanediols or glycerol. *Ind. Eng. Chem. Res.* **2010**, *49*, 4850–4857.
- (2) Makowska, A.; Dyoniziak, E.; Siporska, A.; Szydlowski, J. Miscibility of ionic liquids with polyhydric alcohols. *J. Phys. Chem. B* **2010**, *114*, 2504–2508.
- (3) Deive, F. J.; Rodríguez, A.; Pereiro, A. B.; Shimizu, K.; Forte, P. A. S.; Romão, C. C.; Canongia Lopes, J. N.; Esperança, J. M. S. S.; Rebelo, L. P. N. Phase equilibria of haloalkanes dissolved in ethylsulfate- or ethylsulfonate-based ionic liquids. *J. Phys. Chem. B* **2010**, *114*, 7329–7337.
- (4) Vale, V. R.; Rathke, B.; Will, S.; Schröer, W. Liquid–liquid phase behavior of solutions of 1-dodecyl-3-methylimidazolium bis((trifluoro-

methyl)sulfonyl)amide ($C_{12}\text{mimNTf}_2$) in *n*-alkyl alcohols. *J. Chem. Eng. Data* **2010**, *55*, 4195–4205.

(5) Hefter, G. T. Liquid–Liquid Solubilities. In *The Experimental Determination of Solubilities*; Hefter, G. T., Tomkins, R. P. T., Eds.; Wiley: Chichester, U.K., 2003; Vol. 6, pp 237–256.

(6) Šobr, J.; Hynek, V. Apparatus for objective measurement of liquid–liquid equilibrium. *Sbor. Vys. Sk. Chem.-Tech: Fyz. Chem.* **1976**, *N2*, 125–132.

(7) Becker, F.; Kiefer, M.; Rhensius, P.; Spoerner, A.; Steiger, A. Liquid–liquid equilibria in binary systems of epichlorohydrin and epibromohydrin with *n*-hexane and *n*-heptane. *Z. Phys. Chem.* **1978**, *112*, 139–152.

(8) Singh, R. R.; Van Hook, W. A. The effect of hydrogen/deuterium substitution and pressure on the liquid–liquid equilibrium between cyclohexane and methanol. *J. Chem. Phys.* **1987**, *87*, 6097–6110.

(9) Hefter, G. T.; Barton, A. F. M.; Chand, A. Semi-automated apparatus for the determination of liquid solubilities: Mutual solubilities of water and butan-2-ol. *J. Chem. Soc., Faraday Trans.* **1991**, *87*, S91–S96.

(10) Szydlowski, J.; Rebelo, L. P.; Van Hook, W. A. A new apparatus for the detection of phase-equilibria in polymer solvent systems by light-scattering. *Rev. Sci. Instrum.* **1992**, *63*, 1717–1725.

(11) Ochi, K.; Momose, M.; Kojima, K.; Lu, B. C.-Y. Determination of mutual solubilities in aniline + *n*-hexane and furfural + cyclohexane systems by a laser light scattering technique. *Can. J. Chem. Eng.* **1993**, *71*, 982–985.

(12) Sever, L.; Lieto, J.; Boudehen, A.; Bousquet, J. A novel technique for rapid measurement of liquid–liquid–vapour equilibrium. *Chem. Eng. Sci.* **1998**, *53*, 2587–2594.

(13) Szydlowski, J.; Szykuła, M. Isotope effect on miscibility of acetonitrile and water. *Fluid Phase Equilib.* **1999**, *154*, 79–87.

(14) de Sousa, H. C.; Rebelo, L. P. N. (Liquid + liquid) equilibria of (polystyrene + nitroethane). Molecular weight, pressure, and isotope effects. *J. Chem. Thermodyn.* **2000**, *32*, 355–387.

(15) Bendová, M.; Řehák, K.; Matouš, J.; Novák, J. P. Liquid–liquid equilibrium and excess enthalpies in binary systems methylcyclohexane + methanol and methylcyclohexane + *N,N*-dimethylformamide. *J. Chem. Eng. Data* **2003**, *48*, 152–157.

(16) Heintz, A.; Lehmann, J. K.; Wertz, C. Thermodynamic properties of mixtures containing ionic liquids. 3. Liquid–liquid equilibria of binary mixtures of 1-ethyl-3-methylimidazolium bis((trifluoromethyl)sulfonyl)imide with propan-1-ol, butan-1-ol, and pentan-1-ol. *J. Chem. Eng. Data* **2003**, *48*, 472–474.

(17) Schrödle, S.; Buchner, R.; Kunz, W. Automated apparatus for the rapid determination of liquid–liquid and solid–liquid phase transitions. *Fluid Phase Equilib.* **2004**, *216*, 175–182.

(18) Dean, K. M.; Babayco, C. B.; Sluss, D. R. B.; Williamson, J. C. The accuracy of liquid–liquid phase transition temperatures determined from semiautomated light scattering measurements. *J. Chem. Phys.* **2010**, *133*, No. 074506.

(19) Schwartz, A. J.; Huang, J. S.; Goldberg, W. I. Spinodal decomposition in a binary liquid mixture near the critical point. *J. Chem. Phys.* **1975**, *62*, 1847–1852.

(20) Huang, J. S.; Goldberg, W. I.; Bjerkaas, A. W. Study of phase separation in a critical binary liquid mixture: Spinodal decomposition. *Phys. Rev. Lett.* **1974**, *32*, 921–923.

(21) Easwar, N. Effect of continuous stirring on off-critical and critical samples of a phase-separating binary liquid mixture. *Phys. Rev. Lett.* **1992**, *68*, 186–189.